

NASA TECHNICAL MEMORANDUM

NASA TM-88441

NASA-TM-88441 19860018580

FORMATION OF ASYMMETRIC SEPARATED FLOW PAST SLENDER  
BODIES OF REVOLUTION AT LARGE ANGLES OF ATTACK

Translation of: K vozniknoveniyu nesimmetrichnogo  
otryvnogo obtekaniya tonikh tel vrashcheniya na  
bol'sikh uglakh ataki, IN: Uchenye Zapiski TsAGI,  
Vol. 15, No. 6, 1984, pp. 1-9

FOR REFERENCE

LIBRARY USE

JUL 15 1986

NOT TO BE TAKEN FROM THIS ROOM

LANGLEY RESEARCH CENTER  
LIBRARY, NASA  
HAMPTON, VIRGINIA



NF00978

NATIONAL AERONAUTICS AND SPACE ADMINISTRATION  
WASHINGTON, D.C. 20546 JUNE 1986

## STANDARD TITLE PAGE

1. Report No. NASA TM- 88441	2. Government Accession No.	3. Recipient's Catalog No.	
4. Title and Subtitle FORMATION OF ASYMMETRIC SEPARATED FLOW PAST SLENDER BODIES OF REVOLUTION AT LARGE ANGLES OF ATTACK		5. Report Date June 1986	6. Performing Organization Code
7. Author(s) M.G. Goman, A. N. Khrabrov		8. Performing Organization Report No.	10. Work Unit No.
9. Performing Organization Name and Address Leo Kanner Associates, Redwood City, CA 94063		11. Contract or Grant No. NASW 4005	12. Type of Report and Period Covered Translation
12. Sponsoring Agency Name and Address National Aeronautics and Space Administration Washington D.C., 20546		14. Sponsoring Agency Code	
15. Supplementary Notes Translation of: K vozniknoveniyu nesimmetrichnogo otryvnogo obtekaniya tonkikh tel vrashcheniya na bol'shikh uglakh ataki, IN: Uchenye Zapiski TsAGI, Vol. 15, No. 6, 1984, pp. 1-9 (A86-13429) (ISSN 0321-3429) (UDC 533.6.001.32:629.7.025.73)			
16. Abstract The problem under investigation is about the stationary positions of pairs of vortices of unequal intensity within the flow, behind a cylinder, modeling the asymmetric separation flow around a slender body at high angles of attack. The calculation is being carried out for possible non-symmetric stationary positions of two vortices and their stability is defined in the presence of small perturbations. The bifurcation flow fields are being analyzed in the course of change of the vortex intensity. The possible applications of the obtained results, pertaining to the calculations of the separation flows around a slender body, are being discussed.			
17. Key Words (Selected by Author(s))		18. Distribution Statement Unlimited-Unclassified	
19. Security Classif. (of this report) Unclassified	20. Security Classif. (of this page) Unclassified	21. No. of Pages 15	22. N 86-28052# A86-13429 (ORIGINAL) N-156,147

FORMATION OF ASYMMETRIC SEPARATED FLOW PAST SLENDER BODIES OF  
REVOLUTION AT LARGE ANGLES OF ATTACK

M. G. Goman, A. N. Khrabrov

Central Institute of Aerohydrodynamics

The problem under investigation is about the stationary positions of pairs of vortices of unequal intensity within the flow, behind a cylinder, modeling the asymmetric separation flow around a slender body at high angles of attack. The calculation is being carried out for possible non-symmetric stationary positions of two vortices and their stability is defined in the presence of small perturbations. The bifurcation flow fields are being analyzed in the course of change of the vortex intensity. The possible applications of the obtained results, pertaining to the calculations of the separation flows around a slender body, are being discussed.

/1\*

Of great interest in recent times is the appearance of considerable lateral forces and moments exerted on slender bodies - the missiles, elongated fuselage within the aircraft configuration, at high angles of attack and zero slip angle. The experimental data which has been reviewed in the studies [1, 2] indicate that the appearance of non-symmetric effect at the zero slip angle is associated with the development within a specific range of high angles of attack, of a stationary, asymmetric vortex structure. At small angles of attack, as the flow separates at the tip of a slender body, a symmetric pair of vortex flows is formed, which, as the angle of attack increases, becomes non-symmetric. The appearance of asymmetric vortex structure commences at the angles of attack which exceed the double halfangle of the tip for each particular body [3].

One is familiar with a model [4] which explains the appearance of the lateral load via the development of several vortices, the position

---

\*Numbers in the margin indicate pagination in the foreign text.

of which in space is analogous to the pulse Karmann trail, swept along the longitudinal axis of the body. The reasons however remain unclear as to the cause of the appearance of asymmetry, for example, on the tip of the fuselage, where we have, during the separation flow, only two asymmetric vortices. There are several points of view in this regard. One of them assumes that the cause of the asymmetry is the non-symmetric flow separation which actually results in the development of non-symmetric vortices. According to another point of view, it is assumed that with the increase of the angle of attack, with the concurrent increase in the intensity of the symmetric pair of vortices, at some moment in time this vortex structure becomes unstable, with the development of non-symmetric structure.

The results of the study [5] favor the latter point of view in which the authors, by assigning the a priori symmetric lines of separation at the cone, have obtained the non-symmetric solutions for a set of modeled vortices. /2

In a number of cases, it is permissible to utilize the simplest flow diagram which describes a planar separation flow of an ideal noncompressible liquid around the cylinder. The separation zone in the wake of the cylinder is being modeled by two point vortices with different directional circulation. The possibility of the existence of such established separation flow, utilizing such approach is associated with the cases of stationary position of the vortices. Within the symmetric framework, when the vortices are equal in magnitude but opposite in the directional circulation, such problem was analytically solved in the study [6]. The details of this solution can be found in [7]. In the study [8] this model, on the assumption that the method of planar cross-section is valid, was utilized for the approximate calculation of the symmetric separation flow around a slender body at high angles of attack.

Let us consider this approach in its application to the flow around a cylinder without assuming that the position of the vortices is symmetric and

that the magnitudes of directional circulation are equivalent. Let us assume that in the complex plane of variable  $z=x+iy$ , the position of vortices is assigned by  $z_1$  and  $z_2$  values. The complex flow potential may be obtained by taking into account the vortices with the reverse circulation at the  $1/z_1^*$  and  $1/z_2^*$  points, reflected with respect to the cylinder, the requirement which is necessary to satisfy the no-flow conditions at the cylinder:

$$W(z) = U_\infty \left( z + \frac{1}{z} \right) + \frac{i\Gamma_1}{2\pi} \ln \frac{z - z_1^*}{z - 1/z_1^*} + i \frac{\Gamma_2}{2\pi} \ln \frac{z - z_2^*}{z - 1/z_2^*}, \quad (1)$$

where  $z_1^*$ ,  $z_2^*$  are the complex-conjugated quantities with respect to  $z_1$ ,  $z_2$  and  $\Gamma_1$  and  $\Gamma_2$  are the circulations of vortices. To calculate the speed of vortex movement, one should keep in mind that the vortex exerts no effect on itself and therefore, the complex-conjugated speed of motion of  $j$  vortex ( $j=1, 2$ ) will be expressed as follows:

$$\frac{dz_j^*}{dt} = \lim_{z \rightarrow z_j} \left( \frac{dW}{dz} - i \frac{\Gamma_j}{2\pi} \frac{1}{z - z_j} \right). \quad (2)$$

By introducing the dimensionless coordinates of vortices  $\bar{z}_j = z_j / R$ , the time  $\tau = \frac{U_\infty}{R} t$  and circulatory movement  $\gamma_j = \frac{\Gamma_j}{2\pi U_\infty R}$ , where  $R$  is the cylinder radius and  $U_\infty$  is the speed of incoming flow, we will obtain the relationships which define the vortices speed of motion as a function of their position:

$$\left. \begin{aligned} \frac{d\bar{z}_1^*}{d\tau} &= 1 - \frac{1}{\bar{z}_1^2} - \frac{i\gamma_1}{\bar{z}_1 - 1/\bar{z}_1^*} + \frac{i\gamma_2}{\bar{z}_1 - \bar{z}_2} - \frac{i\gamma_2}{\bar{z}_1 - 1/\bar{z}_2^*}; \\ \frac{d\bar{z}_2^*}{d\tau} &= 1 - \frac{1}{\bar{z}_2^2} + \frac{i\gamma_1}{\bar{z}_2 - \bar{z}_1} - \frac{i\gamma_1}{\bar{z}_2 - 1/\bar{z}_1^*} - \frac{i\gamma_2}{\bar{z}_2 - 1/\bar{z}_2^*}. \end{aligned} \right\} \quad (3)$$

The differential equations (3) describe the position of vortices in time. This autonomous dynamic system is a Hamiltonian one, and the vortex coordinates along the  $O_x$  and  $O_y$  axes may be transformed into the canonically conjugated variables

$$\frac{dx_j}{d\tau} = \frac{1}{\gamma_j} \frac{\partial H}{\partial y_j}, \quad \frac{dy_j}{d\tau} = -\frac{1}{\gamma_j} \frac{\partial H}{\partial x_j}, \quad j=1, 2, \quad (4)$$

/3

where the Hamiltonian system of equations (4)

$$\begin{aligned} H(x_1, y_1, x_2, y_2; \gamma_1, \gamma_2) = & \gamma_1 y_1 \left( 1 - \frac{1}{x_1^2 + y_1^2} \right) + \\ & + \gamma_2 y_2 \left( 1 - \frac{1}{x_2^2 + y_2^2} \right) + \frac{1}{4\pi} \left\{ \gamma_1^2 \ln(x_1^2 + y_1^2 - 1) + \gamma_2^2 \ln(x_2^2 + y_2^2 - 1) + \right. \\ & \left. + 2\gamma_1 \gamma_2 \ln \left[ 1 + \frac{(x_1^2 + y_1^2 - 1)(x_2^2 + y_2^2 - 1)}{(x_1 - x_2)^2 + (y_1 - y_2)^2} \right] \right\} \end{aligned} \quad (5)$$

defines the magnitude of kinetic energy, associated with the relative position of the vortices which is being preserved in the course of their movement.

The stationary positions of the vortices correspond to the specific points within the dynamic system (4) for which

$\frac{dx_j}{d\tau} = \frac{dy_j}{d\tau} = 0$ ,  $j=1, 2$ , and coincide with the critical Hamiltonian point (5):  $\nabla H=0$ . As one can see, the problem of finding the stationary positions of the vortices is reduced to the solution of a system of nonlinear algebraic equations. Within the non-symmetric framework, it is not possible to obtain the analytical solution and therefore the calculation of possible stationary position of the vortices is accomplished numerically.

The effective method of calculating a system of nonlinear equations which are parameter-dependent is the method of continuous extension of the solution.

In the course of a continuous change of one of the parameters, the solution also changes, forming within the expanded space of the phase variables and the parameter a continuous trajectory. The calculation of such a trajectory in selecting its length as an independent variable may be realized by integrating the corresponding system of differential equations, in the presence of starting conditions  $\underline{x} = \underline{x}_0$ ,  $u = u_0$  which are the solution of the system of equations  $\underline{F}(\underline{x}_0, u_0) = 0$ , which we are considering, where  $\underline{x} \in \mathbb{R}^n$ ,  $\underline{F} \in \mathbb{R}^n$ ,  $u \in \mathbb{R}$ . The general concept of using such calculation method can be found in the study [10].

It is also possible to extend the continuous calculation through the points on the trajectory, limiting with respect to the parameter and corresponding to the bifurcation values of the parameter in which one has the sign inversion within the Jacobian system of equations  $\det \left\| \frac{\partial \underline{F}}{\partial \underline{x}} \right\|$  and the directional change of the parameter. This makes it possible to handle the calculations which are ambiguous and obtain the solutions which are continuously interrelated within the expanded space of the variables and the parameter in question.

In calculating the stationary positions of the vortices, we have considered the transformed, dimensionless parameters  $\Gamma$  and  $H$  which will be, according to the mean values of the dimensionless circulatory vortices and the relative magnitude of their asymmetry, as follows:  $\gamma = \frac{1}{2}(\gamma_1 - \gamma_2)$ , and  $\kappa = \frac{\gamma_1 + \gamma_2}{\gamma_1 - \gamma_2}$ . The inverse relationships are also valid  $\gamma_1 = \gamma(1 + \kappa)$ ,  $\gamma_2 = -\gamma(1 - \kappa)$ .

We are considering here the following regions of change in the selected parameters  $\gamma \in (0, \infty)$ ,  $H \in (-1, 1)$ . The equations (3), and also the Hamiltonian (5) will not change when we replace  $H$  by  $-H$  if we replace the  $\tilde{x}_1 = x_2$ ,  $\tilde{y}_1 = -y_2$ ,  $\tilde{x}_2 = x_1$ ,  $\tilde{y}_2 = -y_1$ , which reflect the coordinate position with respect to the  $Ox$  axis. Therefore, for the solution in question, it would suffice to handle only the positive  $H$  parameter. /4

Figure 1 shows the examples for calculation of lines for the stationary position of vortices, as one changes the  $\gamma$  and  $H$  parameters. As the  $\gamma$  parameter changes and  $H=0$ , the stationary positions of the vortices move along the dashed lines which correspond to the symmetric solution. As  $\gamma \rightarrow 0$ , the vortices get closer to the cylinder and as  $\gamma \rightarrow \infty$ , they move towards infinity, along the asymptotes  $y = \pm \frac{1}{2} H$ .

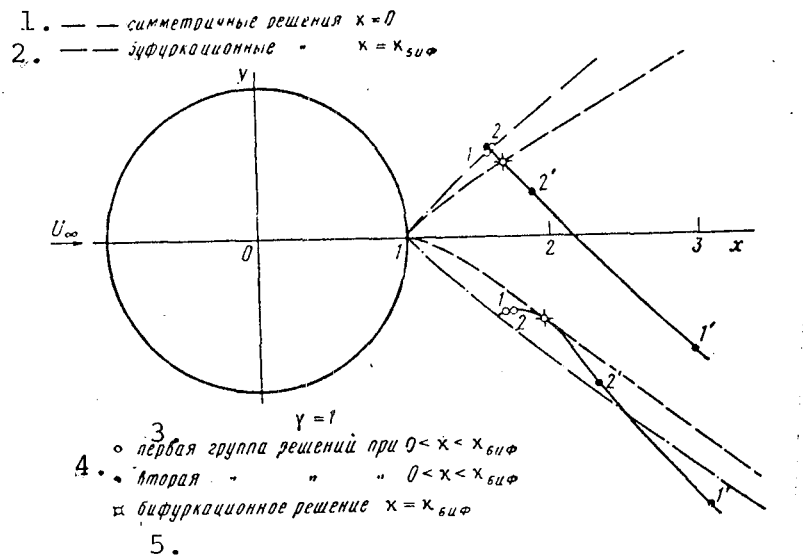


Figure 1.

Key: 1. Symmetric solutions  $H=0$ ; 2. Bifurcational solutions  $H=H_{\text{bif}}$ ; 3. First group of solutions for  $0 < H < H_{\text{bif}}$ ; 4. Second group of solutions  $0 < H < H_{\text{bif}}$ ; 5. Bifurcational solution  $H=H_{\text{bif}}$

The change of  $H$  parameter for a fixed value of  $\gamma=1$  results in the asymmetric displacement of vortices with respect to  $Ox$  axis. There is a limiting - bifurcational value of  $H=H_{\text{bif}}$  parameter, after which, during the continuous extension of the solutions, the  $H$  value begins to decrease. This branch corresponds to the second solutions, existing when  $0 < H < H_{\text{bif}}$ . As  $H$  decreases, the stationary positions of the vortices move toward infinity, being displaced downward along the asymptote  $y = -\frac{1}{2} H$ .

In the limiting case, when  $H \rightarrow 0$ , the vortices approach the stationary position, with the magnitude being the same and the directional circulation being opposite within a uniform flow, since the effect of the cylinder, at some distance from it, is significantly less pronounced.

As the  $H$  values approach  $H_{bif}$ , the stationary position of the vortices pair gets closer and closer ( $l$  and  $l'$  for  $H=0.25H_{bif}$ ,  $2$  and  $2'$  for  $H=0.75H_{bif}$ ) and at  $H=H_{bif}$  - they will merge. Figure 1 shows the positional lines for a pair of vortices when  $H=H_{bif}$  and different values of  $\gamma$  parameter. When  $H>H_{bif}$ , the stationary position of vortices in the cylinder wake is absent. The magnitude of  $H_{bif}$  quantity depends on  $\gamma$  parameter. Keeping in mind the possibility of having the non-symmetric solutions in which  $-H_{bif} < H < 0$ , within the plane of dimensionless circulation of vortices  $\gamma_1$  and  $\gamma_2$ , 1/5 there is a region of parameters for which there will be two different stationary positions of the vortices in the cylinder wake and there also will be a number of parameters in the presence of which there are no stationary positions of vortices in the cylinder wake (Figure 2). The equations (3) will also have some other and special points, when the vortices may be on  $Oy$  axis, either on the same side of the cylinder or on both sides, and will also be found within the flow, in front of the cylinder. These solutions are not being considered since it is known a priori that they cannot be utilized for the description of separation flow.

It is of interest to analyze the stability of motion of the vortices. As has been shown in [6] the symmetric solutions are stable if we are to consider only the symmetric perturbations and are unstable in the presence of small, non-symmetric perturbations, with respect to the stationary position of the vortices.

The analysis of the perturbed motion of the vortices and its stability with respect to the non-symmetric stationary positions were conducted by numerical calculations of the roots of the characteristic equation within the set of linearized equations of

motion (4) in the vicinity of such specific points. The calculation of Jacobian nonlinear equations (4) in such special points, which is the matrix of equations for a linear approximation, is necessary for the development of continuous method in calculating the stationary positions. Therefore, in parallel with the calculation of stationary solutions, it was also necessary to calculate the Jacobi numbers themselves. Since the dynamic system (4) is a Hamiltonian one, the range of these numbers is symmetric with respect to the real and imaginary axes. This property made it possible to control the accuracy in obtaining these numbers, in the course of calculations.

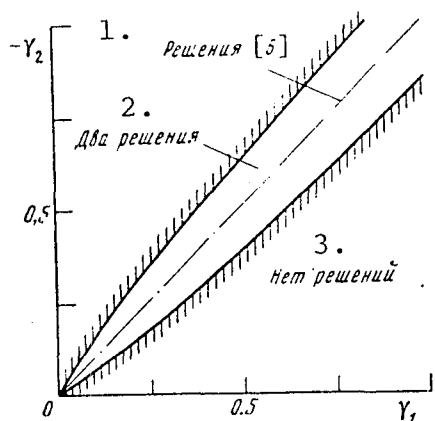


Figure 2.

Key: 1. Solution 6 ; 2. Two solutions;  
3. No solutions

As the circulatory motion increases, the spectrum is preserved qualitatively, approaching the beginning of the coordinates (Figure 3, a).

In the case of the first group of non-symmetric solutions, when  $0 < H < H_{bif}$ , the spectrum of these eigennumbers is analogous to the spectrum of symmetric solutions. As the  $H$  parameter increases, the

The eigennumbers for symmetric solutions are on an imaginary and real axis, and the absolute values of these numbers depends on  $\gamma$  parameter (Figure 3, a). A pair of purely imaginary numbers  $\lambda_{1,2} = \pm \omega$  correspond to the symmetric shape of the vortices perturbations, not increasing in time, and the presence of positive and real number  $\lambda_{3,4} = \pm \xi$  speaks of unstable motions in the presence of non-symmetric perturbations.

eigennumbers move along the imaginary and real axes toward the beginning of the coordinates and at  $H=H_{\text{bif}}$  - we will have the quadruple zero root. Figure 3, b, shows the behavior of the eigennumber  $\alpha$  as a function of  $H$  at  $\gamma=2$ . /6

The other group of non-symmetric solutions qualitatively has another spectrum, which can be seen in Figure 3, b. The equilibrium positions also are not stable, but the instability nature is of oscillatory character and this is due to the presence of complex-conjugated pair of eigennumbers  $\lambda_{1,2}=\xi \pm i\omega$ , part of which is positive and real. As the  $H$  parameter increases, the eigennumbers first increase and then begin to decrease down to zero at  $H=H_{\text{bif}}$  (see Figure 3, b).

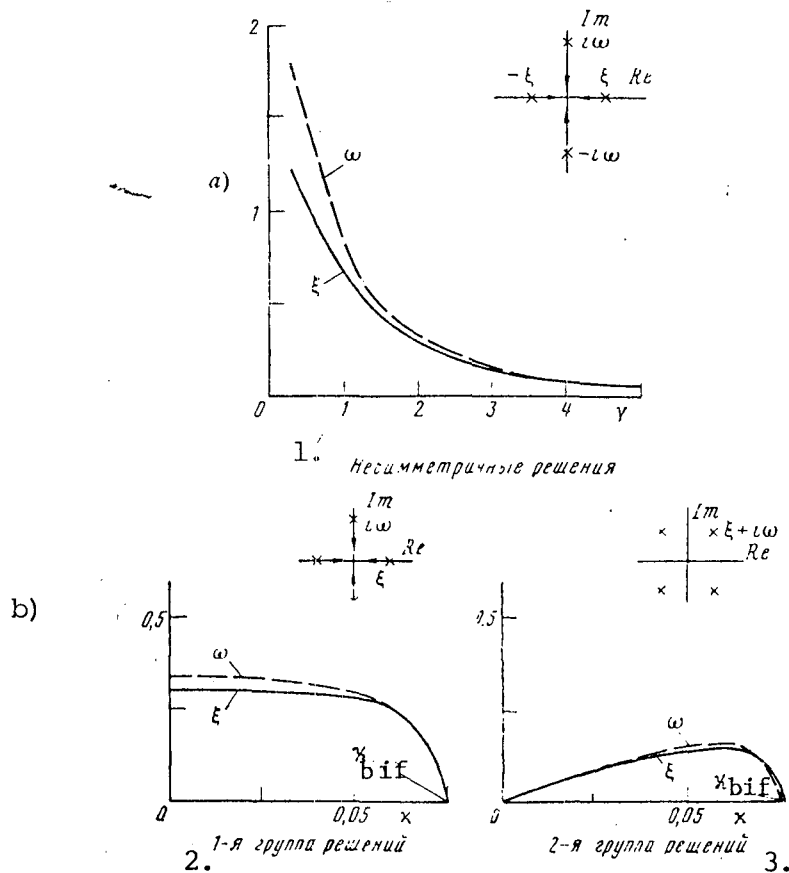


Figure 3.

Key: 1. Non-symmetric solution; 2. 1st group of solutions;  
3. 2nd group of solutions

The stability considerations of the stationary separation flow within the framework of such simple planar system, unquestionably, cannot be transposed on the tridimensional separation flows, even within the range of the theory of a slender body. Nonetheless, this general concept as to the stability may turn out to be useful in considering more complex flow systems.

The different depiction of the flow fields will correspond to the stationary conditions in the equations (4). To comprehend the physical meaning of the obtained stationary solutions, it is necessary to have the general idea about them. Therefore, it was necessary to calculate and construct the most significant flow lines which define the general nature of the wake. Among these lines, one should first of all mention the flow lines along which the flow braking to zero /7 velocity takes place. Such points may be found on the cylinder surface as well as within the free flow. Their number and position define the qualitative structure of the flow field.

The magnitude of the flow function which is an imaginary part of the complex potential  $W(z)$  (1):  $\psi(x, y) = \text{Im } W(z)$  remains constant along the flow lines. In constructing the special flow lines, the values of the flow function at the point of the flow braking was determined, after which it was possible to construct the level of the lines along which the flow function will be computed. This made it possible to construct the flow lines which form within the flow field the saddle points.

We shall consider different values of  $\gamma$  and  $H$  parameters, in the presence of which the stationary flow around the object is possible. /8 The constructed flow fields are shown in Figure 4. The upper series shows the cases of symmetric cylinder wake flow and a pair of vortices in the wake for different circulatory  $\gamma(H=0)$ . The cases which are considered topologically are analogous and are characterized by the presence of two centers at the points of the positioning of vortices, for half-saddles A, B, C, D on the cylinder and one saddle E within

the flow wake. In the symmetric case, all saddle points are at the same level of the flow function  $\psi=0$ .

As the symmetry appears  $H>0$ , the E point is elevated to a certain level  $\psi=\psi_0>0$ , and as a result of this, in the wake of the flow, one will observe a flow gap which is shaded in the picture. The C and D half-saddles begin to approach each other and as the bifurcation state approaches  $H=H_{\text{bif}}$ , they will merge, forming one, degenerated half-saddle F. When the asymmetry parameter H increases, the E saddle first will be elevated, and the flow gap will expand. In the course of further increase of H, the gap begins to decrease. At the level of bifurcation  $H=H_{\text{bif}}$  and small  $\gamma$ , the merging of C and D points will take place when the level of the flow function at the point E is still positive. For large  $\gamma$  in the case of bifurcation solution at the point E the negative flow function will be displaced and the flow gap will be observed on the other side of the cylinder. There is an intermediate value of  $\gamma=\gamma^*\approx 0.57$ , when the bifurcation solution will have no flow gap: a zero flow line will pass through the saddle E. In the case when  $\gamma>\gamma^*$ , the disappearance of the flow gap (the zero value of the flow function at the point E) occurs when the value of H is close to  $H_{\text{bif}}$ . The picture of such wake flow for such H is shown in the column for  $\gamma>\gamma^*$  among the first non-symmetric solutions.

The second non-symmetric solutions are topologically different from the first ones. They are characterized by the presence of two points of G and E saddle type within the flow, and the flow lines here are forming two isolated and closed regions, separated by the flow gap. Let us note that the structural difference in the first and second types of flows within the framework of non-symmetric solutions is accompanied by different stability spectra, applicable to these solutions.

Let us consider the flows with closed vortex regions, adjoining the cylinder. In the case of small  $\gamma$  parameter, there is only one

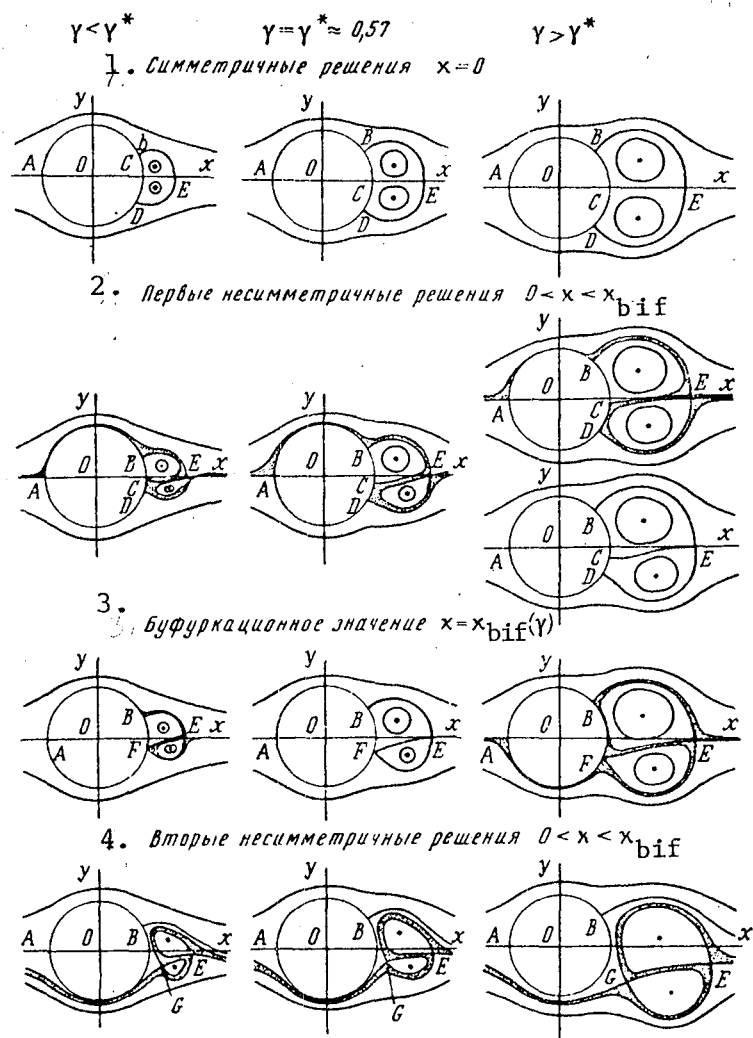


Figure 4.

Key: 1. Symmetric solution; 2. First non-symmetric solutions;  
 3. Bifurcation value; 4. Second non-symmetric solutions

symmetric solution. For the circulatory levels of  $\gamma > \gamma^*$  - there are three solutions without flow gaps: one symmetric and two non-symmetric - for  $H > 0$  and  $H < 0$ . It should be noted that the non-symmetric solutions, in a certain sense, are less "stable," something which is manifested in the lower positive real root (see Figure 3, b) when compared to the symmetric solution.

The study [11] presents the experimental data in regard to the flow field around the cylindrical body, with the ogive nose cone, in the course of appearance of non-symmetric separation flow. The non-symmetric position of vortices is associated with the separation of the flow line which emerges from the saddle point, within the flow, away from the body. In this case, it embraces one of the vortices and is moved away along the flow gap. The flow fields observed in [11] are similar to those which are considered in Figure 4.

If one is to assume that in a real wake flow, the viscous flow effect will prevent the flow gaps, of all possible solutions, we could select the flows with closed vortex regions. At the tip of a slender body, where the circulatory motion of the vortices is small, something which is being observed experimentally, we have a symmetric vortex structure. As one moves further away from the nose, the vortex circulatory activity increases, and at a certain distance, the transition towards one of the non-symmetric solutions may become possible.

The study [9] (page 102) which involved the slender rotational bodies, shows the dimensionless intensity of vortices  $\Gamma_v / 2\pi\alpha V_0 R$  as a function of the dimensionless parameter  $\alpha(x-x_0)/R$  which are introduced for considerations of similarity ( $\Gamma_v$  is the circulation of vortices,  $\alpha$  is the angle of attack,  $V_0$  is the speed of incoming flow,  $R$  is the radius of rotating body,  $x$  is the coordinate along the body,  $x_0$  is the coordinate of the point at which the vortex commences to move from the tip of the body). /9

Within the framework of the flow diagrams under consideration and utilizing the method of planar bodies,  $U_\infty = V_0 \alpha$ . By assuming that  $x_0 \approx 0$ , and by replacing  $x/R$  by  $1/\epsilon$ , where  $\epsilon$  is the half-cone angle of the nose for a given body, the relationships presented in [9] may be represented as a linear dependence  $\gamma = \frac{k\alpha}{\epsilon}$ , where  $k \approx 0.3$  is a constant, empirically determined from the curve.

If the body is such that along all its length the dimensionless circulation of vortices  $\gamma < \gamma^*$ , the appearance of asymmetric vortex structure, utilizing these assumptions, is impossible. If however, within a certain range of the angles of attack, the intensities of vortices toward the end of the body become greater than  $\gamma^*$ , one may be faced with asymmetry. This may take place when  $\gamma = \frac{k\alpha}{\epsilon} > \gamma^*$  or if the angles of attack  $\alpha > \frac{\gamma^*}{k} \epsilon$ . By substituting into this relationship the critical value of  $\gamma^*$  parameter  $\gamma^* \approx 0.57$  and the empirical value of  $k \approx 0.3$ , we will end up with the development of asymmetric vortex structure at the tail end of the body, in the form of  $\alpha > 1.9\epsilon$ . This correlates with the experimental data, indicating that the lateral loads will begin to appear when the angles of attack are greater than the double half-cone angle of a given body.

## REFERENCES

1. Ericsson, L.E. and J.P. Reding, "Review of vortex-induced asymmetric loads, Part I," Z. Flugwiss. Weltraumforsch, No. 5, Heft 3 (1981).
2. Ericsson, L.E. and J.P. Reding, "Review of vortex-induced assymtric loads, Part II," Z. Flugwiss. Weltraumforsch, No. 5, Heft 6 (1981).
3. Keener, E.R. and G.T. Chapman, "Onset of aerodynamic side forces at zero sideslip on symmetric forebodies at high angles of attack," AIAA Paper, 74, 770 (1974).
4. Thomson, K.D. and D.E. Morrison, "The spacing, positions and strength of vortices in the wake of slender cylindrical bodies at large incidence," J. of Fluid Mech. 50, 4 (1971).
5. Dyer, D.E., S.P. Fiddes and J.H.B. Smith, "Asymmetric vortex formation from cones at incidence - a simple inviscid model," Aeronautical Quaterly 33, 4 (1982).
6. Föppl, L, "Vortex movement in the cylinder wake," Sitzb. d. k. Bäyr. Akad. d. Wiss. (1913).
7. Lamb, G., Gidrodinamika [Hydrodynamics] Gostekh Press, Moscow, Leningrad, 1947.
8. Veykhs, D., "Approximate calculation of the trajectories of vortices, in the wake of slender bodies at an angle of attack," Rakettaya tekhnika i kosmonavtika 18/11 (1980).
9. Nilsen, J. Aerodinamika oupravlyayemykh snaryadov [Aerodynamics of the Guided Missiles] Oboron Press, 1962.
10. Davidenko, D.F., "On one of the new methods of numerical solution for the sytems of nonlinear equations," DAN SSSR [Reports of the Academy of Sciences of the USSR] 88/4 (1953).
11. Yonta, W.G., A.B. Wardlaw and Naval, Jr., "The secondary separation region on a body at high angles of attack," AIAA Paper, N 82-0343.

Received by Editorial Board on June 13, 1983

**End of Document**